arXiv:1405.1867v3 [hep-th] 2 Sep 2014

Ultraviolet fixed point and massive composite particles in TeV scales

She-Sheng Xue*

ICRANeT, Piazzale della Repubblica, 10-65122, Pescara,

Physics Department, University of Rome "La Sapienza", Rome, Italy

We present a further study of the dynamics of high-dimension fermion operators attributed to the theoretical inconsistency of the fundamental cutoff (quantum gravity) and the parity-violating gauge symmetry of the standard model. Studying the phase transition from a symmetry-breaking phase to a strong-coupling symmetric phase and the β-function behavior in terms of four-fermion coupling strength, we discuss the critical transition point as a ultraviolet-stable fixed point where a quantum field theory preserving the standard model gauge symmetry with composite particles can be realized. The form-factors and masses of composite particles at TeV scales are estimated by extrapolating the solution of renormalization-group equations from the infrared-stable fixed point where the quantum field theory of standard model is realized and its phenomenology including Higgs mass has been experimentally determined. We discuss the probability of composite-particle formation and decay that could be experimentally verified in the LHC by measuring the invariant mass of relevant final states and their peculiar kinetic distributions.

PACS numbers: 12.60.-i,12.60.Rc,11.30.Qc,11.30.Rd,12.15.Ff

Introduction. The parity-violating (chiral) gauge symmetries and spontaneous/explicit breaking of these symmetries for the hierarchy of fermion masses have been at the center of a conceptual elaboration that has played a major role in donating to mankind the beauty of the standard model (SM) for particle physics. The Nambu-Jona-Lasinio model (NJL) [1] of four-fermion interactions at high energies and its effective counterpart, the Higgs model [2] of fermion-boson Yukawa interactions at low energies, provide an elegant description for the electroweak symmetry breaking and intermediate gauge boson masses. After a great experimental effort for many years, the ATLAS [3] and CMS [4] experiments have recently shown the first observations of a 126 GeV scalar particle in the search for the Standard Model Higgs boson at the LHC. This far-reaching result begins to shed light on this most elusive and fascinating arena of fundamental particle physics.

It is an important issue to study the dynamics at high-energy scale that originates the high-dimensional operators of fermion fields. The strong technicolor dynamics of extended gauge theories

*Electronic address: xue@icra.it

at the TeV scale was invoked [5, 6] to have a natural scheme incorporating the relevant four-fermion operator (1) of the NJL type. We here present a brief introduction that the origin of high-dimensional operators of all fermion fields is due to the quantum gravity at the Planck length ($a_{\rm pl} \sim 10^{-33}\,{\rm cm}$, $\Lambda_{\rm pl} = \pi/a_{\rm pl} \sim 10^{19}\,{\rm GeV}$). Studying the quantum Einstein-Cartan theory in the framework of Regge calculus, we calculated [7] the minimal length ($\approx 1.2\,a_{\rm pl}$) of discrete space-time, which provides a natural regulator for local quantum field theories of particles and gauge interactions. On the other hand, based on low-energy observations of parity violation, the SM Lagrangian was built in such a way as to preserve the exact chiral-gauge-symmetries $SU_L(2)\otimes U_Y(1)$ that are accommodated by elementary left-handed fermions and right-handed fermions. However, a profound result, in the form of a generic no-go theorem [8], tells us that there is no consistent way to straightforwardly transpose on a discrete space-time the bilinear fermion Lagrangian of the continuum SM theory in such a way as to exactly preserve the chiral gauge symmetries. We are led to consider at least quadrilinear fermion interactions to preserve the chiral gauge symmetries. As an example, the four-fermion operator in the Einstein-Cartan theory can be obtained by integrating over static torsion fields at the Planck scale [9]. The very-small-scale structure of space-time and high-dimensional operators of fermion fields must be very complex as functions of the space-time spacing $\tilde{a}$ and the gravitational gauge-coupling $g_{\rm grav}$ between fermion fields and quantum gravity at the Planck scale. As the running gravitational gauge-coupling $g_{\rm grav}(\tilde{a})$ is approaching to its ultraviolet (UV) stable critical point $g_{\rm grav}^{\rm crit}$ for $\tilde{a} \to a_{\rm pl}$ [10], the physical scale $\Lambda = \Lambda[g_{\rm grav}(\tilde{a}), \tilde{a}]$ ($\Lambda^{-1} \gg \tilde{a}$) satisfies the renormalization-group (RG) equation in the scaling region of the UV-stable fixed point, where the irrelevant high-dimensional operators of fermion fields are suppressed at least by $\mathcal{O}(\Lambda/\Lambda_{\rm pl})$; only the relevant operators receive anomalous dimensions and become effectively renormalizable dimension-4 operators at the high-energy scale Λ.

On the other hand, these relevant operators can be constructed on the basis of the phenomenology of SM at low-energies. In 1989, several authors [11–13] suggested that the symmetry breakdown of SM could be a dynamical mechanism of the NJL type that intimately involves the top quark at the high-energy scale Λ. Since then, many models based on this idea have been studied [14]. The top-quark and Higgs-boson masses were supposed to be achieved by the RG equations in the scaling region of the infrared (IR) stable fixed point [6, 12, 13]. In the following discussions, we adopt the BHL model of an effective four-fermion operator [13]

$$L = L_{\rm kinetic} + G(\bar{\psi}_L^{ia} t_{Ra})(\bar{t}_R^b \psi_{Lib}), \quad G \sim 1/\Lambda^2 \tag{1}$$

in the context of a well-defined quantum field theory at the high-energy scale Λ.

For the reason that the four-fermion interaction may be due to quantum gravity at the Planck scale where all fermions should be on an equal footing, we generalized [15] the Lagrangian (2) to

$$\begin{aligned} L &= L_{\rm kinetic} + G(\bar{\psi}^{ia}_L\psi_{Rja})(\bar{\psi}^{jb}_R\psi_{Lib}) + \text{terms}, \\ &= L_{\rm kinetic} + G(\bar{\psi}^{ia}_L t_{Ra})(\bar{t}^b_R\psi_{Lib}) + G(\bar{\psi}^{ia}_L b_{Ra})(\bar{b}^b_R\psi_{Lib}) + \text{terms}, \end{aligned} \tag{2}$$

where a, b and i, j are the color and flavor indexes of the top and bottom quarks, the $SU_L(2)$ doublet $\psi^{ia}_L = (t^a_L, b^a_L)$ and the singlet $\psi^a_R = t^a_R, b^a_R$ are the eigenstates of the electroweak interaction, and addition terms for the first and second quark families can be obtained by substituting $t \to u, c$ and $b \to d, s$ [16]. Moreover, we showed that the less numbers of Goldstone modes (positive energy) are, and the smaller total energy of the system is, as a result the minimal dynamical symmetry breaking (1) is an energetically favorable configuration (ground state) of the quantum field theory with high-dimension operators of all fermion fields at the cutoff Λ.

It was shown [17–19] that if the four-fermion coupling $G(\mu)$ is larger than a critical value $G_{\rm crit}$, and the energy scale μ is larger than a threshold energy scale $\mathcal{E}_{\rm thre}$, the weak-coupling symmetry-breaking phase transits to the strong-coupling symmetric phase where massive composite particles are formed fully preserving the chiral gauge symmetries of SM, and the parity-symmetry is restored. In Ref. [20], we found a unique solution to the RG equation in the symmetry-breaking phase, which indicates the threshold energy scale $\mathcal{E}_{\rm thre} \approx 4.27\,\text{TeV}$ and the form-factor of composite Higgs boson $\tilde{Z}_H(\mathcal{E}_{\rm thre}) \approx 1.1$, corresponding to the Higgs-boson mass $m_{_H} \approx 126.7\,\text{GeV}$ and top-quark mass $m_t \approx 172.7\,\text{GeV}$. As a consequence, these masses and the pseudoscalar decay constant f_π can be obtained without drastically fine-tuning the four-fermion coupling.

In this Letter, utilizing the BHL model (1) in the symmetry-breaking phase, we numerically solve the RG equations of the SM with an infrared boundary conditions fixed by the top-quark and Higgs-boson masses recently measured, and obtain the form-factor of composite Higgs boson, increasing as the energy scale μ increasing up to the energy threshold $\mathcal{E} \approx 5\,\text{TeV}$, at which the Higgs-boson quartic coupling $\bar{\lambda}(\mathcal{E})$ vanishes. This is different from the BHL result obtained by imposing the compositeness conditions of the form-factor vanishing at high-energy cutoff scale Λ. Moreover, we show that in the symmetry-breaking phase the $\beta(G)$-function is positive near to an infrared-stable fixed point for the SM, while the $\beta(G)$-function is negative in the strong-coupling symmetric phase, where the composite Higgs boson combines with an elementary fermion to form a massive composite fermion. This implies that the critical point of the second-order phase transition should be a UV-stable fixed point. The result $\mathcal{E} \approx 5\,\text{TeV}$ from the solution to RG-equations infers the energy scale in the scaling region of the UV-stable fixed point. As a result, we estimate the

spectra of massive composite particles and discuss the high-energy collider signatures of these composite particles, which could be identified by the resonance in invariant mass and particular kinematic distribution of final states measured.

The IR-stable fixed point and symmetry-breaking phase. In this phase, the quantum field theory (1) contains the massive spectra of top quark and composite Higgs boson. Employ the "large N_c-expansion", i.e., keep GN_c fixed and construct the theory systematically in powers of $1/N_c$. At the lowest order of one fermion-loop contribution, one obtains the gap equation for top-quark mass $m_t \neq 0$

$$\frac{1}{G_c} - \frac{1}{G} = \frac{1}{G_c}\left(\frac{m_t}{\mathcal{E}}\right)^2 \ln\left(\frac{\mathcal{E}}{m_t}\right)^2 > 0, \tag{3}$$

for $G \gtrsim G_c \equiv 8\pi^2/(N_c\mathcal{E}^2)$, where $\mathcal{E} \approx \mathcal{E}_{\rm thre}$ characterizes the energy scale of restoring symmetries for $G \gtrsim G_{\rm crit}$. In Eq. (3), considering m_t as a running energy scale μ, we can approximately obtain the running coupling

$$G(\mu) \approx G_c\left[1 - \left(\frac{\mu}{\mathcal{E}}\right)^2 \ln\left(\frac{\mathcal{E}}{\mu}\right)^2\right]^{-1}, \tag{4}$$

and the β-function

$$\beta(G) \equiv \mu\frac{dG}{d\mu} \;\approx\; 2\frac{G^2}{G_c}\left(\frac{\mu}{\mathcal{E}}\right)^2\left[1 + \ln\left(\frac{\mathcal{E}}{\mu}\right)^2\right] > 0, \tag{5}$$

for $G_{\rm crit} > G \gtrsim G_c$ and $\mathcal{E} > \mu \gtrsim v$, where v is the electroweak scale. The positive β-function of Eq. (5) indicates that G_c is an IR-stable fixed point, $G \to G_c + 0^+$ as $\mu \to v$. Here we ignore the behavior of the functions $G(\mu)$ and $\beta(G)$ for $G \to G_c + 0^-$ in the weak-coupling symmetric phase ($G < G_c$), therefore G_c should be regarded as a "quasi" IR-stable fixed point. To represent the behavior of the $\beta(G)$-function discussed up to now, we sketch in Fig. 1 the positively increasing curve "I" of the $\beta(G)$-function departing from $G = G_c$, where the coupling $G(\mu)$ increases as the energy scale μ increases in the range $v \lesssim \mu < \mathcal{E}$.

The scaling region of the IR-stable fixed point. The full induced effective Lagrangian of the low-energy SM in the scaling region of the IR-stable fixed point takes the form [13]

$$\begin{aligned} L \;&=\; L_{\rm kinetic} + g_{t0}(\bar{\Psi}_L t_R H + {\rm h.c.}) + \Delta L_{\rm gauge} \\ &+\; Z_H|D_\mu H|^2 - m_{_H}^2 H^\dagger H - \frac{\lambda_0}{2}(H^\dagger H)^2, \end{aligned} \tag{6}$$

and all renormalized quantities received fermion-loop contributions are defined with respect to the low-energy scale μ. The conventional renormalization $Z_\psi = 1$ for fundamental fermions and the

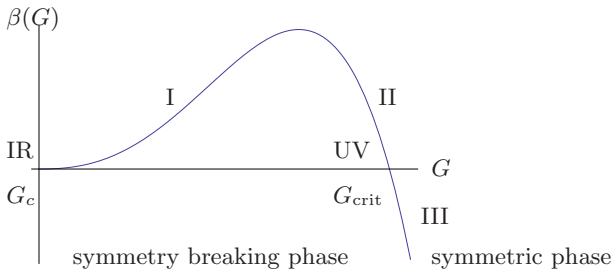

FIG. 1: This is a sketch to qualitatively show the behavior of the β-function in terms of the four-fermion coupling G. We indicate the quasi IR-stable fixed point G_c and a possible UV-stable fixed point $G_{\rm crit}$, the latter separates the symmetry-breaking phase (positive $\beta(G)$-function) from the symmetric phase (negative $\beta(G)$-function). We also indicate the positive parts "I" (increasing) and "II" (decreasing), as well as the negative part "III" of the $\beta(G)$-function.

unconventional wave-renormalization (form factor) $\tilde{Z}_H$ for composite Higgs bosons are adopted [13]

$$\tilde{Z}_H(\mu) = \frac{1}{\bar{g}_t^2(\mu)},\ \bar{g}_t(\mu) = \frac{Z_{HY}}{Z_H^{1/2}} g_{t0}; \quad \tilde{\lambda}(\mu) = \frac{\bar{\lambda}(\mu)}{\bar{g}_t^4(\mu)},\ \bar{\lambda}(\mu) = \frac{Z_{4H}}{Z_H^2}\lambda_0, \tag{7}$$

where Z_{HY} and Z_{4H} are proper renormalization constants of the Yukawa-coupling and quartic coupling in Eq. (6). In the scaling region of the IR-stable fixed point where the SM of particle physics is realized, we utilize the full one-loop RG equations for running couplings $\bar{g}_t(\mu^2)$ and $\bar{\lambda}(\mu^2)$

$$16\pi^2 \frac{d\bar{g}_t}{dt} = \left(\frac{9}{2}\bar{g}_t^2 - 8\bar{g}_3^2 - \frac{9}{4}\bar{g}_2^2 - \frac{17}{12}\bar{g}_1^2\right)\bar{g}_t, \tag{8}$$

$$16\pi^2 \frac{d\bar{\lambda}}{dt} = 12\left[\bar{\lambda}^2 + (\bar{g}_t^2 - A)\bar{\lambda} + B - \bar{g}_t^4\right], \quad t = \ln\mu \tag{9}$$

where one can find A, B and RG equations for running gauge couplings $g_{1,2,3}^2$ in Eqs. (4.7), (4.8) of Ref. [13]. In this IR scaling region, the electroweak scale $v \approx 239.5\,\text{GeV}$ and the mass-shell conditions

$$m_t = \bar{g}_t(m_t)v/\sqrt{2}, \quad m_{_H}^2/2 = \tilde{\lambda}(m_{_H})v^2, \tag{10}$$

are set in. Using the experimental values of M_w, M_z, $g_{1,2,3}^2$, $\cdots$ including the top-quark and Higgs-boson masses,

$$m_{_H} = 126 \pm 0.5\,\text{GeV}; \quad m_t = 172.9 \pm 0.8\,\text{GeV}, \tag{11}$$

we adopt (10) as an infrared boundary condition to integrate the RG equations (8) and (9) so as to uniquely determine the functions of $\tilde{Z}_H(\mu)$ and $\tilde{\lambda}(\mu)$ (see Fig. 2), as well as the values of $\tilde{Z}_H(\mathcal{E})$ and

the energy scale $\mathcal{E}$ for $\tilde{\lambda}(\mathcal{E}) = 0$. We examine the variations of $\tilde{Z}_H(\mathcal{E})$ and $\mathcal{E}$ values corresponding to the uncertainties in experimental measurements (11). The results are reported in Tab. I and the maximal variations are

$$\mathcal{E} = 5.1 \pm 0.7 \text{ TeV}, \quad \tilde{Z}_H = 1.26 \pm 0.02. \tag{12}$$

This indicates that as a unique solution to the RG equations (8) and (9), how much variations of $\mathcal{E}$ and $\tilde{Z}_H(\mathcal{E})$ in high energies correspond to the variations of boundary values (10) in low energies, due to the uncertainties of top-quark and Higgs-boson masses (11). Note that the uncertainties of gauge couplings and boson masses have not been taken in account in this calculations.

It is important to compare and contrast our study with the BHL one [13]. In both studies, the definitions of all physical quantities are identical, the same RG equations (8) and (9) are used for running Yukawa and quartic couplings as well as gauge couplings. However, the different boundary conditions are adopted. We impose the infrared boundary condition (10) with (11) that are known nowadays, to uniquely determine the solution of the RG equations, and values of the form-factor $\tilde{Z}_H(\mathcal{E}) \neq 0$ and high-energy scale $\mathcal{E}\,[\tilde{\lambda}(\mathcal{E}) = 0]$, as shown in Fig. 2 $\tilde{Z}_H(\mu)$ $[\tilde{\lambda}(\mu)]$ monotonically increases (decreases) as the energy scale μ increases up to $\mathcal{E}$. Both experimental m_t and $m_{_H}$ values were unknown in the early 1990s, in order to find low-energy values m_t and $m_{_H}$ close to the IR-stable fixed point, BHL [13] imposed the compositeness conditions $\tilde{Z}_H(\Lambda) = 0$ and $\tilde{\lambda}(\Lambda) = 0$ for different values of the high-energy cutoff Λ as the boundary condition to solve the RG equations. As a result, m_t and $m_{_H}$ values (Table I in Ref. [13]) were obtained, and we have reproduced these values. However, these BHL results are radically different from the present results of Eqs. (11), (12) and Fig. 2, showing that the composite Higgs boson actually becomes a more and more tightly bound state, as the energy scale μ increases, and eventually combines with an elementary fermion to form a composite fermion in the symmetric phase (see next section). This phase transition to the symmetric phase is also indicated by $\tilde{\lambda}(\mu) \to 0^+$ as $\mu \to \mathcal{E} + 0^-$ at which the 1PI vertex function Z_{4H} in Eqs. (7), (6) vanishes.

The Yukawa coupling $\bar{g}_t(\mu) = [\tilde{Z}_H(\mu)]^{-1/2} < 1$ and quartic coupling $\bar{\lambda}(\mu) = \tilde{\lambda}(\mu)\bar{g}_t^4(\mu) < 0.15$ for $m_{_H} < \mu < \mathcal{E}$, as shown in Fig. 2. This consistently indicates that the RG equations (8) and (9) derived from perturbative calculations for small couplings $\bar{g}_t(\mu)$ and $\bar{\lambda}(\mu)$ are reliable to obtain the numerical results $\tilde{Z}_H(\mathcal{E})$ and $\mathcal{E}$ of Eq. (12). The non-vanishing form-factor $\tilde{Z}_H(\mu)$ means that after conventional wave-function and vertex renormalizations $Z_H^{1/2} H \to H$, $Z_{HY} g_{t0} \to g_{t0}$ and $Z_{4H}\lambda_0 \to \lambda_0$ [see Eqs. (6) and (7)], the composite Higgs boson behaves as an elementary particle. However, its effective Yukawa coupling $\bar{g}_t(\mu)$ and quartic coupling $\bar{\lambda}(\mu)$ decrease with the energy

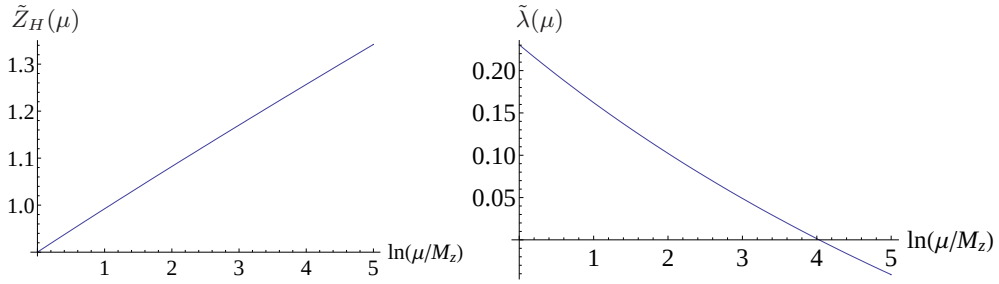

FIG. 2: Using all experimentally measured quantities at low energies, we numerically solve the RG equations (8), (9) and boundary conditions (10), (11) to uniquely determine the functions $\tilde{Z}_H(\mu)$ and $\tilde{\lambda}(\mu)$ of Eq. (7) in terms of the energy scale $\mu > M_z$. Since $\tilde{\lambda}(\mathcal{E})$ cannot be negative, otherwise the total energy of the system would not be bound from below, we numerically determine the values (12) of $\mathcal{E}$ and $\tilde{Z}_H(\mathcal{E})$ by demanding $\tilde{\lambda}(\mathcal{E}) = 0$.

m_H \ m_t	$172.9 + 0.8\,\mathrm{GeV}$	$172.9 - 0.8\,\mathrm{GeV}$	$172.9\,\mathrm{GeV}$
$126 + 0.5\,\mathrm{GeV}$	$\tilde{Z}_H = 1.24; \mathcal{E} = 4.9\,\mathrm{TeV}$	$\tilde{Z}_H = 1.28; \mathcal{E} = 5.8\,\mathrm{TeV}$	$\tilde{Z}_H = 1.26; \mathcal{E} = 5.3\,\mathrm{TeV}$
$126 - 0.5\,\mathrm{GeV}$	$\tilde{Z}_H = 1.24; \mathcal{E} = 4.6\,\mathrm{TeV}$	$\tilde{Z}_H = 1.28; \mathcal{E} = 5.4\,\mathrm{TeV}$	$\tilde{Z}_H = 1.27; \mathcal{E} = 5.0\,\mathrm{TeV}$
$126\,\mathrm{GeV}$	$\tilde{Z}_H = 1.24; \mathcal{E} = 4.8\,\mathrm{TeV}$	$\tilde{Z}_H = 1.28; \mathcal{E} = 5.7\,\mathrm{TeV}$	$\tilde{Z}_H = 1.26; \mathcal{E} = 5.1\,\mathrm{TeV}$

TABLE I: The center values of top-quark and Higgs masses are chosen as $m_t = 172.9\,\mathrm{GeV}$ and $m_H = 126\,\mathrm{GeV}$. This table shows the variations of the theoretical values of $\tilde{Z}_H(\mathcal{E})$ and $\mathcal{E}$, corresponding to the variations of experimental values of top-quark and Higgs masses (11).

scale μ increasing in the range $m_H < \mu < \mathcal{E}$. This would have some effects on the rate or cross-sections of the composite Higgs boson decay or other relevant processes. In future work, it will be examined by comparison to electroweak precision data if these effects could be low-energy collider signatures that would tell this scenario apart from the SM with an elementary Higgs boson.

The UV-stable fixed point and strong-coupling symmetric phase. From the results (12), we can have some insight into the energy threshold $\mathcal{E}_{\mathrm{thre}}$ and the form-factor $\tilde{Z}_H(\mathcal{E}_{\mathrm{thre}})$ of composite particles in the strong-coupling symmetric phase, where the composite Higgs boson and an elementary fermion are bound to form a three-fermion state to restore the symmetry. In the strong-coupling limit $Ga^{-2} \gg 1$, where $a \equiv (\pi/\Lambda)$, the theory (2) is in the strong-coupling symmetric phase [17, 18]. This was shown by scaling $\psi(x) \to \psi(x) = a^2 g^{1/4} \psi(x)$ and $g \equiv G/a^4$

$(ga^2 \gg 1)$, writing the action (2) as

$$S_{\rm kinetic} \;=\; \frac{1}{2ag^{1/2}}\sum_{x,\mu}\bar{\psi}(x)\gamma_\mu\partial^\mu\psi(x), \quad \partial^\mu \equiv \delta_{x,x+a_\mu}-\delta_{x,x-a_\mu} \tag{13}$$

$$S_{\rm int} \;=\; \sum_x\Big[(\bar{\psi}^{ia}_L t_{Ra})(\bar{t}^b_R\psi_{Lib})+(\bar{\psi}^{ia}_L b_{Ra})(\bar{b}^b_R\psi_{Lib})\Big], \tag{14}$$

and using the strong coupling (hopping) expansion in powers of $1/g^{1/2}$ to calculate two-point functions of composite fermion and boson fields. Using the first term (t_{Ra}-channel) in Eq. (14), in the lowest non-trivial order (one-hopping step) we obtained (see Section 4 in Ref. [17]) the propagator of the composite Dirac fermions: $SU_L(2)$-doublet $\mathbf{\Psi}^{ib}_D=(\psi^{ib}_L,\mathbf{\Psi}^{ib}_R)$ and $SU_L(2)$-singlet $\mathbf{\Psi}^b_D=(\mathbf{\Psi}^b_L,t^b_R)$, where the renormalized composite three-fermion states are:

$$\mathbf{\Psi}^{ib}_R=(Z^S_R)^{-1}(\bar{\psi}^{ia}_L t_{Ra})t^b_R\,; \quad \mathbf{\Psi}^b_L=(Z^S_L)^{-1}(\bar{\psi}^{ia}_L t_{Ra})\psi^b_{iL}, \tag{15}$$

with mass $M=2ga$ and form-factor $Z^S_{R,L}=Ma$, the latter is a generalized wave-function renormalization of composite fermion operators. The composite bosons ($SU_L(2)$-doublet) are (see Section 5 in Ref. [17])

$$H^i=[Z^S_H]^{-1/2}(\bar{\psi}^{ia}_L t_{Ra}), \quad \mu^2_{_H}=\frac{4}{N_c}\left(g-\frac{2N_c}{a^2}\right), \tag{16}$$

where $[Z^S_H]^{1/2}$ and $\mu_{_H}$ respectively are the form-factor and mass of composite bosons. Eq. (16) confirms the spontaneous symmetry breaking $SU(2)\to U(1)$ by the effective mass term $\mu^2_{_H}HH^\dagger$ changing its sign from $\mu^2_{_H}>0$ to $\mu^2_{_H}<0$, $\mu^2_{_H}=0$ gives rise to the critical coupling $G_{\rm crit}$, whose exact value however has to be calculated by non-perturbative numerical simulations. In the lowest non-trivial order of the strong-coupling expansion, the positive contribution to the 1PI vertex of the self interacting term $(HH^\dagger)^2$ is suppressed by $(1/g)^2$. Note that the same calculations based on the second term (b_{Ra}-channel) in Eq. (14) lead to the composite particles represented by Eqs. (15)-(16) with the replacement $t_{Ra}\to b_{Ra}$, carrying the different quantum numbers of the $U_Y(1)$ gauge group. These discussions are also the same for the first and second quark families by substituting the $SU_L(2)$ doublet (t_{La},b_{La}) into (u_{La},d_{La}) or (c_{La},s_{La}) and singlet t_{Ra} into u_{Ra} or c_{Ra}, as well as singlet b_{Ra} into d_{Ra} or s_{Ra} in Eq. (2).

In the symmetry breaking phase and the scaling region of the IR-stable fixed point, we know the symmetries, particle spectrum (fermions and bosons) and all relevant renormalizable operators of the SM at low energies [see Eq. (6)]. In the strong-coupling symmetric phase, the three-fermion states (15) are the bound states of the composite boson $H^i=(\bar{\psi}^{ia}_L t_{Ra})$ and elementary fermion t^b_R (ψ^b_{iL}), and the SM chiral-gauge symmetries are fully preserved by the massive composite fermions

$\mathbf{\Psi}_D^{ib}$ and $\mathbf{\Psi}_D^{b}$, as well as their vector-like couplings to γ, $W^{\pm}$, Z^0 and gluon gauge bosons, consequently leading to the parity-symmetry restoration.

We attempt to discuss the possible behaviors "II" and "III" of the $\beta(G)$-function in the strong-coupling regimes (see Fig. 1). To see how the strong coupling g depends on the energy-momentum, we need to calculate the corrections from more "hopping" steps to the form-factor ($Z^S_{R,L} = Ma$) and mass ($M = 2ga$) of composite fermions (15). In the analogy of calculations presented in the Appendix B of Ref. [17] and discussions presented in Ref. [18], these corrections can be approximately calculated by using the train approximation for each fermion of Eq. (15),

$$[Z^S_{R,L}(p)/aM]^{-1} \approx (1+\sigma+\sigma\sigma+\cdots)^3 = \left(\frac{1}{1-\sigma}\right)^3, \tag{17}$$

$$\sigma(p) = -\frac{2}{(g^{1/2})^4}\left(\frac{\gamma_\nu p^\nu}{p^2}\right)\int_{k,q}^{\Lambda}\frac{\gamma_\mu(p+q)^\mu}{(p+q)^2}\frac{(k^2-q^2/4)}{(k-q/2)^2(k+q/2)^2}, \tag{18}$$

where p is the energy-momentum of composite particles and $\sigma(p)$ is represented by Fig. 3 and its negative sign is attributed to *two* fermion loops. We rewrite Eq. (18) as

$$\sigma(p) = -\frac{2}{(g^{1/2})^4}\left(\frac{\gamma_\nu p^\nu}{p^2}\right)\gamma_\mu p^\mu \Lambda^4 \Phi(p^2/\Lambda^2) = -\frac{2\pi^4}{G^2\Lambda^4}\Phi(p^2/\Lambda^2), \tag{19}$$

where the dimensionless function $\Phi(p^2/\Lambda^2)$ is a Lorentz scalar. Numerical calculations confirm that the function $\Phi(p^2/\Lambda^2)$ is positive and finite, monotonically decreases as p^2/Λ^2 increases. As a result, the corrected form-factor $Z^S_{R,L}(p) = Ma[1-\sigma(p)]^3$, leading to the effective running coupling

$$\mathcal{G}(p) \approx \mathcal{G}\left[1+\frac{6}{\mathcal{G}^2}\Phi(p^2/\Lambda^2)\right], \quad \mathcal{G} \equiv G\times(\Lambda/\pi)^2 \tag{20}$$

and the β-function

$$\beta(G) = p^2\frac{\partial \mathcal{G}(p)}{\partial p^2} \approx \frac{6}{\mathcal{G}}\frac{\partial \Phi(p^2/\Lambda^2)}{\partial \ln(p^2/\Lambda^2)} < 0. \tag{21}$$

This result indicates a negative β-function and $\beta \to 0^-$ in the strong-coupling limit. Recall that in the QED case the analogous contribution of *one* fermion loop to the wave-function renormalization constant Z_3 is positive, the β-function is positive, i.e., $\beta_{\rm QED} \approx e^3/12\pi^2 > 0$. On the basis of the $\beta(G)$-function being positive and negative respectively in the weak-coupling symmetry-breaking phase and strong-coupling symmetric phase, as sketched as "I" and "III" in Fig. 1, we infer there must be at least one zero-point of the $\beta(G)$-function, i.e., $\beta(G_{\rm zero}) = 0$ and $\beta'(G_{\rm zero}) < 0$. At this zero-point $G_{\rm zero}$, the positive $\beta(G)$-function "II" turns to the negative β-function "III". This zero-point $G_{\rm zero}$ is a UV-stable fixed point.

The scaling region of the UV-stable fixed point. We are not able to determine $G_{\rm zero}$, however we expect $G_{\rm zero} \simeq G_{\rm crit}$ for the reason that a UV-stable fixed point should be the candidate of

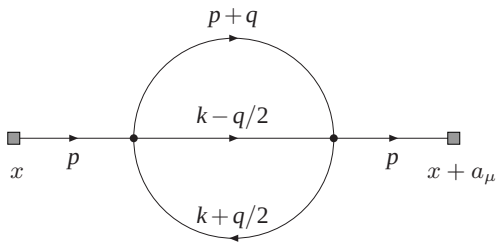

FIG. 3: The Feynman diagram represents the contribution $\sigma(p)$ from the one-hopping step of each fermion field in Eq. (15).

critical point $G_{\rm crit}$ for the second-order phase transition. It is known that in the neighborhood of the critical point $G_{\rm crit}$, the correlation length ξ/a of the theory goes to infinity, leading to the scaling invariance, i.e., the renormalization-group invariance. In this scaling region, the running coupling $G(a/\xi)$ can be expanded as a series,

$$G(a/\xi) \;=\; G_{\rm crit}\left[1 + a_0(a/\xi)^{1/\nu} + \mathcal{O}[(a/\xi)^{2/\nu}]\right] \to G_{\rm crit} + 0^+, \tag{22}$$

for $a/\xi \ll 1$, leading to the β-function

$$\beta(G) \;=\; (-1/\nu)(G - G_{\rm crit}) + \mathcal{O}[(G - G_{\rm crit})^2] < 0\,. \tag{23}$$

The correlation length ξ follows the scaling law

$$\xi \;=\; c_0 a \exp\int^G \frac{dG'}{\beta(G')} = \frac{c_0 a}{(G - G_{\rm crit})^\nu}, \tag{24}$$

where the coefficient $c_0 = (a_0 G_{\rm crit})^\nu$ and critical exponent ν need to be determined by non-perturbative numerical simulations. Analogously to the electroweak scale $v = 239.5\,{\rm GeV}$ sets in the scaling region of the IR-stable fixed point G_c, the physical scale $\mathcal{E}_\xi \equiv \xi^{-1}$ sets in the scaling region of the UV-stable fixed point $G_{\rm crit}$. This implies the masses of composite particles

$$\mathcal{M} \approx \mathcal{E}_\xi = \xi^{-1}, \tag{25}$$

and the running coupling $G(\mu)|_{\mu\to\mathcal{E}_{\rm thre}+0^+} \to G_{\rm crit}$,

$$G(\mu) \simeq G_{\rm crit}\left[1 - \frac{1}{\nu}\ln\left(\frac{\mu}{\mathcal{E}_\xi}\right)\right]^{-1}, \quad \mu/\mathcal{E}_\xi = \xi/(a a_0^\nu) > 1\,, \tag{26}$$

and the scale μ indicates the energy transfer between constituents inside composite particles. In the scaling region of the UV-stable fixed point, all one-particle-irreducible (1PI) functions $\Gamma[\mu, G(\mu)]$ of the quantum field theory (2) at the high-energy scale Λ evolve to irrelevant or relevant 1PI

functions, as the energy scale μ increases. The irrelevant 1PI functions are suppressed by powers of $(\mathcal{E}_\xi/\Lambda)^n$ and thus decouple from the theory. Instead, the relevant 1PI functions follow the scaling law, therefore are effectively dimension-4 and renormalizable, for example the propagators of composite fermions and bosons and their vector-like coupling vertexes to the SM gauge bosons.

The propagators of these composite particles have poles and residues that respectively represent their masses and form-factors. As long as their form-factors are finite, these composite particles behave as elementary particles. As discussed in Sections V and VI of Ref. [18], when the energy scale μ decreases to the energy threshold $\mathcal{E}_{\rm thre}$ and $G(\mu) \to G_{\rm crit}(\mathcal{E}_{\rm thre})$, the phase transition occurs from the symmetric phase to the symmetry breaking phase, all three-fermion and two-fermion bound states (poles) dissolve into their constituents, which are represented by three-fermion and two-fermion cuts in the energy-momentum plane, as their form-factors and binding energy vanish [21]. The propagators of these composite particles give their mass-shell conditions

$$E_{\rm com} = \sqrt{p^2 + \mathcal{M}^2} \approx \mathcal{M}, \quad \text{for} \;\; p \ll \mathcal{M} \tag{27}$$

where the mass $\mathcal{M}$ contains the negative binding energy $-\mathcal{B}[G(\mu)]$ and positive kinetic energies $\mathcal{K}$ of their constituents. The energy threshold $\mathcal{E}_{\rm thre}$ is determined by $\mathcal{B}[G(\mu)]_{\mu\to\mathcal{E}_{\rm thre}} \to \mathcal{K}$ and vanishing form-factors of composite particles.

As required by minimizing total energy of the system discussed for Eq. (2), only the three-fermion bound state (15) (top-quark channel) dissolves into a Higgs boson and a top quark (boson-fermion cut), and dynamical symmetry-breaking takes place. The form-factors (15) and (16) $Z^S_{L,R} \approx [Z^S_H]^{1/2}[Z_\psi]^{1/2}$ approach to the form-factor $[\tilde{Z}_H]^{1/2}$ of Eqs. (7) and (12), where $[Z_\psi]^{1/2} = 1$ for the conventional renormalization of elementary fermion fields. This means that the energy-threshold $\mathcal{E}_{\rm thre}$ corresponds the energy scale of dynamical symmetry breaking. When the energy scale μ decreases below the energy threshold $\mathcal{E}_{\rm thre}$, i.e., $\mu < \mathcal{E}_{\rm thre}$, in the symmetry-breaking phase, the RG equations take the theory away from the UV fixed point towards the scaling region of the IR fixed point where the low-energy SM of particle physics is realized. On the basis of these discussions, we advocate the following relation for (i) the energy scale $\mathcal{E} \approx 5$ TeV of Eq. (12) extrapolated by the RG equations from the scaling region of the IR fixed point, (ii) the energy threshold $\mathcal{E}_{\rm thre}$ corresponding to the phase transition for dynamical symmetry breaking and (iii) the characteristic energy scale $\mathcal{E}_\xi$ setting in the scaling region of the UV fixed point

$$\mathcal{E} \approx \mathcal{E}_{\rm thre} \lesssim \mathcal{E}_\xi \ll \Lambda, \quad \mathcal{E} \approx 5\,{\rm TeV}. \tag{28}$$

Since $\mathcal{E}$ is determined by $\tilde{\lambda} \to 0^+$, this strongly indicates the occurrence of the phase transition at $\mathcal{E} \approx \mathcal{E}_{\rm thre}$ discussed below Eq. (16), otherwise the theory would run into an instability ($\tilde{\lambda} \sim 0^-$)

beyond $\mathcal{E}$. The approximate $\mathcal{E}$-value (12) is obtained by using the RG-equations (8) and (9), which do not give the positively decreasing curve "II" of the $\beta(G)$-function sketched in Fig. 1. Nevertheless, we gain some physical insight into the symmetry-breaking scale $\mathcal{E}_{\rm thre}$ and composite particle masses $\mathcal{M} \approx \mathcal{E}_\xi \gtrsim 5\,{\rm TeV}$.

Compared with the SM in the IR-stable scaling region, the composite field theory in the UV-stable scaling region has the same chiral gauge symmetries (quantum numbers) and couplings to gauge bosons ($\gamma, W^\pm, Z^0$ and gluon), but the different vector-like spectra and 1PI vertexes, apart from massive particles being comprised by SM elementary ones. These composite particles on mass-shells behave as if they were elementary, as long as their form-factors are finite. The weak and strong interactions (2) bring us into two distinct domains. This is reminiscent of the QCD dynamics: asymptotic free quark states near to a UV fixed point and bound hadron states near to a possible IR fixed point.

Experiments. These composite particles should be produced by high-energy quarks and gauge bosons, if the center-of-mass energy ($\sqrt{s}$) of pp collisions in the LHC is larger than their mass $\mathcal{M}$ or the threshold energy $\mathcal{E}_{\rm thre}$. These could be experimentally verified by possibly observing the resonances in the invariant masses ($\mathcal{M}_{\rm inv}$) and kinematic distributions of final channels measured. We first discuss the most probable channel of producing the composite particles (15) of the first quark family by pp collisions in the LHC. The elementary quarks $(u,d)_{L,R}$ are approximately massless with definite L- and R-chirality at TeV scales. Instead, formed Dirac composite particles, e.g., $[\bar{u}_{Lb}, (\bar{u}^a_L u_{Ra}) u^b_R]$ or $[\bar{d}_{Lb}, (\bar{u}^a_R d_{La}) u^b_R]$, are very massive, non-relativistic (almost static) in the center-of-mass (CM) frame. The most probable channel of producing them is via the interaction (2) of the first quark family, rather than via gauge interactions. Thus we estimate the cross-section of composite-particle formation $\sigma_{\rm com} \sim 1/\mathcal{M}^2$. If the CM energy $\sqrt{s} \gtrsim \mathcal{M}$ or $\mathcal{E}_{\rm thre}$, composite particles are not stable and appear as resonances ($\mathcal{M}_{\rm inv} \approx \mathcal{M}$), and final states are two quarkonia/mesons, each of them decays to two jets in opposite directions (four-jets event) and the jet energy is about $\mathcal{M}/4$. The decay rate (inverse lifetime) of static composite particles $\tau^{-1}_{\rm com} \sim \mathcal{M}$ in the CM-frame. The quarkonia-channels $\bar{u}u$ and $\bar{d}d$ have the same branching ratio, which is the one-half of branching ratio of the meson-channel $\bar{u}d$. Analogously the bosonic composite particles (16) decay to the final state of quarkonium or meson that forms two jets in opposite directions (two-jets event) and the jet energy is about $\mathcal{M}/2$. The same discussions apply for the second and third quark families, but quark pairs are most probably produced by two gluons with the cross-section $\sigma_{\rm com} \sim \alpha_s^2/\mathcal{M}^2$. The composite particle (15) comprising top quark is related to the resonant channel with final states: a Higgs boson of energy $\sim \mathcal{M}/2$ and a $\bar{t}\,t$ pair, the latter becomes two

jets of energy $\sim \mathcal{M}/4$ each, and three momenta are in the same plane with almost 120° angular separation between them, rather than the four-jets event for the first and second quark families. This implies that the strong interaction (2) would give rise not only to bound states, but also to peculiar kinematics of their decays, which are very different from the SM gauge interactions. Thus we would expect that the SM background should be more or less zero. In currently scheduled LHC runs for next 20 years, the integrated luminosity will go from $10\,\text{fb}^{-1}$ up to $10^3\,\text{fb}^{-1}$ and the CM energy $\sqrt{s}$ from 7 TeV up to 14 TeV, then the event number of composite particles can be estimated by $\sigma_{\text{com}} \times 10^{1-3}\text{fb}^{-1} \sim 10^{5-7}$ for the (u,d) family, $\sim 10^{3-5}$ for the (c,s) and (t,b) families, assuming $\mathcal{M} \sim 5\,\text{TeV}$.

To end this Letter, we advocate that it is deserved to theoretically study the particle spectrum and symmetry of the strong-coupling theory (2) at the UV fixed point by non-perturbative numerical simulations, meanwhile experimentally verify the resonances of composite particles with the peculiar kinematic distributions of their final states in LHC.

Acknowledgment. Author is grateful to Prof. Hagen Kleinert for discussions on the IR- and UV-stable fixed points of quantum field theories, to Prof. Zhiqing Zhang for discussions on the LHC physics.

---

[1] Y. Nambu and G. Jona-Lasinio, Phys. Rev. 122 (1961) 345.

[2] F. Englert, R. Brout, Phys. Rev. Lett. 13 (1964) 321;
P. W. Higgs, Phys. Lett. 12 (1964) 132; Phys. Rev. Lett. 13 (1964) 508; Phys. Rev. 145 (1966) 1156;
G. S. Guralnik, C. R. Hagen, T. W. B. Kibble, Phys. Rev. Lett. 13 (1964) 585; and T. W. B. Kibble, Phys. Rev. 155 (1967) 1554.

[3] ATLAS Collaboration, Phys. Lett. B 716 (2012) 1.

[4] CMS Collaboration, Phys. Lett. B 716 (2012) 30-61.

[5] C. T. Hill, Phys. Lett. B266 (1991) 491 and *ibid* B345 (1995) 483; Phys. Rev. D87 (2013) 065002.

[6] C. T. Hill, Phys. Rev. D24, 691 (1990); C. T. Hill, C. N. Leung, S. Rao, Nucl. Phys. B262, 517, (1985); J. Bagger, S. Dimopoulous, E. Masso, Phys. Rev. Lett. 55 920 (1985).

[7] S.-S. Xue, Phys. Lett. B682 (2009) 300, and Phys. Rev. D82, 064039 (2010).

[8] H.B. Nielson and M. Ninomiya, Nucl. Phys. B185 (1981) 20, *ibid* B193 (1981) 173, *Phys. Lett.* **B105** (1981) 219, *Int. J. Mod. Phys.* **A6** (1991) 2913.

[9] S.-S. Xue, Phys. Lett. B665 (2008) 54,
H. Kleinert, "Multivalued Fields", (World Scientific, Singapore, 2008), ISBN-13 978-981-279-171-9.

[10] S.-S. Xue, Phys. Lett. B711 (2012) 404.

[11] Y. Nambu, in Proceedings of the 1989 Workshop on Dynamical Symmetry Breaking, edited by T. Muta and K. Yamawaki (Nagoya University, Nagoya, Japan, 1990);
V.A. Miranski, M. Tanabashi and K. Yamawaki, *Mod. Phys. Lett.* **A4** (1989) 1043; *Phys. Lett.* **B221** (1989) 117.

[12] W. J. Marciano, Phys. Rev. Lett. 62, (1989) 2793.

[13] W. A. Bardeen, C. T. Hill and M. Lindner, *Phys. Rev.* **D41** (1990) 1647.

[14] G. Cvetic, Rev. Mod. Phys. 71 (1999) 513-574;
C. T. Hill, E. H. Simmons, Phys. Rept. 381 (2003) 235-402; *Erratum-ibid.* 390 (2004) 553-554.

[15] S.-S. Xue, Phys. Lett. B721 (2013) 347, references therein.

[16] Eq. (2) has been generalized to the lepton section, see S.-S. Xue, arxiv.org/abs/1405.1867 (v1)

[17] S.-S. Xue, Nucl. Phys. B486 (1997) 282, *ibid* B580 (2000) 365, references therein.

[18] S.-S. Xue, Phys. Rev. D 61 (2000) 054502, references therein.

[19] S.-S. Xue, J. Phys. G, Nucl. Part. Phys. 29 (2003) 2381, references therein.

[20] S.-S. Xue, Phys. Lett. B727 (2013) 308, references therein.

[21] S. Weinberg, Phys. Rev. **130** 776 (1963), **131**, 440 (1963), **133**, B232 (1963), **137**, B672 (1965).